

# Semi-Autonomous Interventional Manipulation using Pneumatically Attachable Flexible Rails\*

C. D’Ettorre, A. Stilli, G. Dwyer, J. B. Neves, M. Tran, D. Stoyanov

**Abstract**—During laparoscopic surgery, tissues frequently need to be retracted and mobilized for manipulation or visualisation. State-of-the-art robotic platforms for minimally invasive surgery (MIS) typically rely on rigid tools to interact with soft tissues. Such tools offer a very narrow contact surface thus applying relatively large forces that can lead to tissue damage, posing a risk for the success of the procedure and ultimately for the patient. In this paper, we show how the use of Pneumatically Attachable Flexible (PAF) rail, a vacuum-based soft attachment for laparoscopic applications, can reduce such risk by offering a larger contact surface between the tool and the tissue. *Ex vivo* experiments are presented investigating the short- and long-term effects of different levels of vacuum pressure on the tissues surface. These experiments aim at evaluating the best trade-off between applied pressure, potential damage, task duration and connection stability. A hybrid control system has been developed to perform and investigate the organ repositioning task using the proposed system. The task is only partially automated allowing the surgeon to be part of the control loop. A gradient-based planning algorithm is integrated with learning from teleoperation algorithm which allows the robot to improve the learned trajectory. The use of Similar Smooth Path Repositioning (SSPR) algorithm is proposed to improve a demonstrated trajectory based on a known cost function. The results obtained show that a smoother trajectory allows to decrease the minimum level of pressure needed to guarantee active suction during PAF positioning and placement.

## I. INTRODUCTION

Robot-Assisted Minimal Invasive Surgery (RAMIS) has rapidly increased in popularity both in the number of surgical procedures performed and in the surgical specialties that use it. Over 1M [1] were performed using RAMIS last year driven by the enhanced ability to perform delicate and precise MIS by controlling laparoscopic tools through small incisions. In MIS to increase the operative space, the anatomical cavity is inflated (creating a pneumoperitoneum in the case of the abdomen) before inserting the ports through which tools are passed into the anatomical cavity. Tissue and organ dissection, retraction and repositioning are usually required in order to treat the targeted anatomy. Usually, the tools which are not actively operating in the task, are used to retract the tissue in the surrounding space, (Fig.1 - left

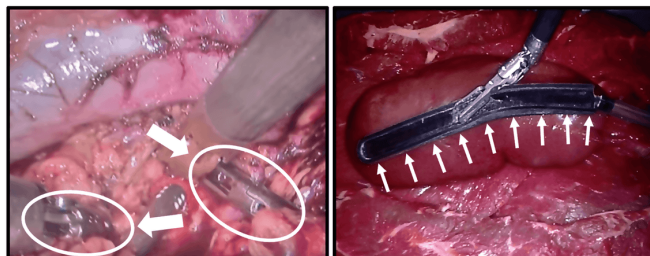


**Fig. 1:** On the left side, a frame from a clinical intra-abdominal RAMIS surgical operation is shown [3]. There are two tools actively operating and two others, white circled, are being used to retract the tissue. On the right side, there is the proof of concept in an *ex vivo* experimental environment to show how the pneumatic rail can improve the interaction with the tissue during the execution of the task.

side). This operation can be difficult since there is no haptic feedback and high pressures applied in localized points could cause inadvertent damage to tissue. Moreover, the contact surface area between the tool and the tissue or organ being retracted is small, necessitating frequent repositioning due to the inherent mobility of tissues and slippage.

We aim to test a new design for a soft rail [2] applied to the repositioning task. The use of a Pneumatically Attachable Flexible rail (PAF Rail) could potentially represent a new concept tool for the repositioning and stabilisation of internal organs during interventions. The design of the rail also enables the spread of the suction force applied to the tissue over a larger surface (Fig.1 - right side) thanks to the suction cups’ line. The PAF design also allows incorporation of automation concepts not currently available in clinical practice. By combining current technology and PAF rails with different control schemes, it may be possible to overcome some of the technically difficult surgical sub-tasks by providing useful adjuncts to the current robotic tools. Automation of surgical sub-tasks could reduce surgeons’ fatigue and optimise performance while decreasing operating time. Tissue retraction and organ repositioning represent good candidates for this purpose. This work aims to verify how the PAF rail can be used during surgery by aiding repositioning or retraction, and how this task can be partially automatized supporting the surgeon as part of the control loop.

Teleoperation along with kinesthetic learning, as any form of learning from demonstration, represent efficient [4] and intuitive [5] teaching methods. They allow experts, in our case surgeons, to communicate tasks to a robotic agent [6]

\*This research is supported by the Wellcome / EPSRC Centre for Interventional and Surgical Sciences (WEISS) and from the EPSRC Impact Acceleration Accounts (IAA) 201720: Discovery-to-use funding.

C. D’Ettorre, A. Stilli, G. Dwyer and D. Stoyanov are with the Centre for Medical Image Computing (CMIC) and the Department of Computer Science, Wellcome/ EPSRC Centre for Interventional and Surgical Sciences (WEISS), University College London, London W1W 7EJ, UK {c.d’ettorre@ucl.ac.uk}

J. B. Neves and M. Tran are with the Research Department of Surgical Biotechnology, Division of Surgery and Interventional Science, University College of London, Royal Free Hospital, London NW3 2QG, UK

avoiding some of the complexity and challenges in robot decision making [5]. Surgeons have the domain knowledge about what constitutes a successful task but modelling this knowledge can be challenging. Moreover, the robot is expected to improve on the trajectory subject to the environment and to this end a hybrid control scheme is introduced to compute the planning of the path for picking and positioning the PAF rail over the target organ, and to improve the demonstrated trajectory from during repositioning tasks.

## II. RELATED WORK

This work relates to contributions on tissue retraction and organ repositioning, learning from demonstration and efforts involving the *pick and place* task.

### A. Tissue Retraction and Organ Repositioning

This research focuses only on surgical procedures and not on percutaneous interventions. Early applications for tissue stabilization were addressed in cardiac operations [7], [8], [9]. This operation is characterized by a highly dynamic environment, hence it becomes important to have a device which is able to stabilize the tissue, allowing the surgeon to operate. These systems are designed for thoracotomy with an insertion point of 10 cm running in the intercostal space but they do not fit laparoscopic general surgery requirements. In [10], the device uses negative pressure (vacuum) applied through a surgical instrument, to fix the position of a portion of the surface of the beating heart so that the surgical procedure can be performed more easily. More recently, devices compatible with MIS have been developed [11], [12]. In [11], the new device is based on a cup with an operating channel inside, designed mainly for uterine surgery. A vacuum pump is coupled to provide suction to the cup via vacuum conduit. In use, the surgical instrument is maneuvered such that the cup is located around a target area of tissue. All the surgical steps take place inside the cup volume which fairly restricts the operating space. A bowl retractor is introduced in [12]. This system is compatible with the da Vinci platform since it can be inserted in a collapsed position through the surgical trocars. Once inside, the expanded position allows organ retraction. All the systems listed above aim to stabilize the tissue around the operating site, constraining the space surrounding the tool. In our case, the PAF rail does not restrict the operative space and can enhance surgeons task management.

### B. Learning from Demonstration

The mapping between the world state and action represents one of the most important learning problem for many robotics applications. Argall et al's work provides an extensive review of the topic [13].

The use of expert demonstrations has been applied to learn successful trajectories in dynamic environments [14]. In [15], a framework based on Gaussian Mixture Models (GMMs) was used for motion generation. Van den Berg et al. [16] analyzed the suturing, where an iterative method is used to learn a trajectory and execute it at a

higher speed than the demonstrated one. The work has been extended in [17], where dynamic changes are faced in an industrial environment. Human demonstration can also be generalized to similar and unseen initial conditions using principles of fluid dynamics [18] and [19] non-rigid registration techniques. In [20], another surgical sub-task application, multilateral cutting, is analyzed in the frame of observational learning. Learning from demonstration (Lfd) broadly classifies all those approaches where demonstrated trajectories are modified to generalize test situations [21], [5]. The presented work aims to allow the robot to improve an already successful trajectory over a specific cost function, without the need of searching the entire trajectories space. The framework presented, modifies the path itself to improve over an arbitrary cost function, instead of improving the execution time of the trajectory based on a more energy-efficient solution as done in [22].

### C. Pick and Place Tasks

This work aims to safely manipulate tissues with the use of the PAF rail during a surgical procedure. According to [23], the robot manipulation of objects can be divided into 4 phases: *Pre-grasp Approach*, *Grasp Acquisition*, *Post-grasp Transportation*, and *Placement*. In the *pre-grasp approach* step, the arm directs towards the object. To achieve this purpose a motion planning followed by its execution is used. In the *Grasp acquisition* phase, the gripper makes contact with the object. The third step, *Post-grasp transportation* is performed after the object is grasped, and it consists of moving the object from one position to another. In the final *placement* phase, the object is placed in the target position. Grasping and manipulation represent two important topics especially in the industrial area, where many related works are present. [24], [25] are two of the several works that show the simulation of a robotic arm for object manipulation. Zhu et al. [26] analyzed the manipulation of flexible cables and how a robot can imitate human abilities. More recently [27], the topic of dexterous grasping has been combined with mobile manipulator moving forward more complex task execution. In the surgical area, Alambegi et al. [28] proposed a control scheme that is able to manipulate, with a continuous robot, a tissue without knowing its properties. In [29], the grasping and manipulation of the suturing needle represents a key problem previous to the suturing process. In all these contributions, the authors mainly focus on one step of the four phases. Instead on our work, as a first proof of concept, we had to face all the different steps.

## III. PROBLEM STATEMENT AND CONTRIBUTION

The overall task of pick and place and tissue repositioning can be summarized as follows: during the *pre-grasp approach* the tool approaches the rail inserted from the surgeons assistant through the auxiliary hole. In the *grasp acquisition* the tip of the robotic instrument engages with the grasping site of the rail. *Post-grasp transportation*, the PAF rail is moved toward the target organ, and it reaches the *placement* when it is correctly in suction with the surface allowing

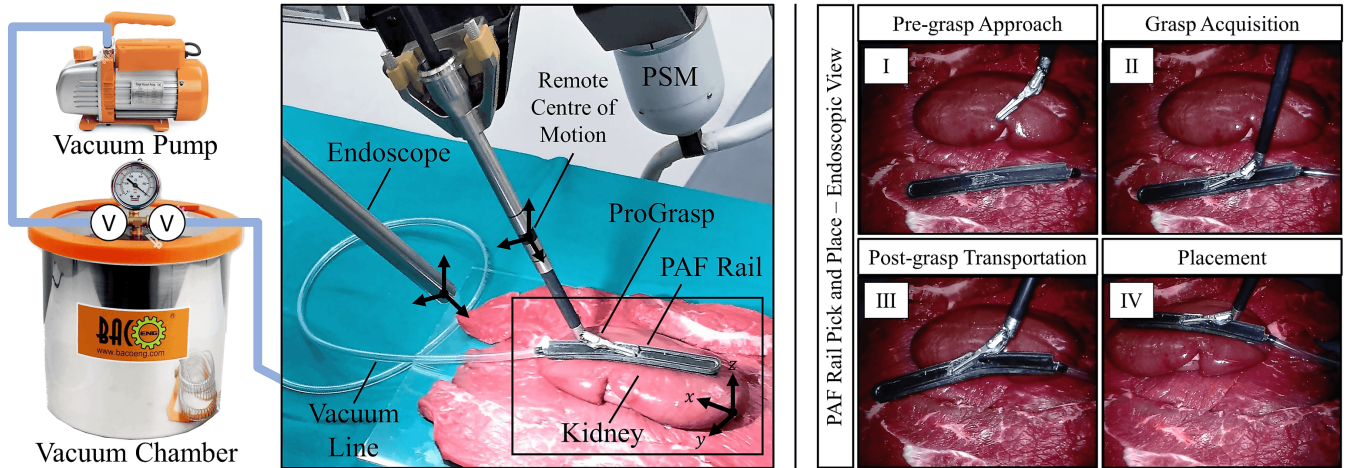


**Fig. 2:** On the left side, representation of the experimental setup. The robotic arm (Patient Side Manipulator - PSM) is equipped with the pro-grasp tool. The remote center of motion reference frame is represented in black. The stereo endoscope is pointing towards the operating workspace characterized by an *ex vivo* porcine kidney and the PAF rail. The PVC vacuum line connects the rail to the vacuum chamber connected to a single stage vacuum pump. The workspace reference frame axes are represented in black next to the kidney. On the right side, representation of the four steps of pick and locate task. I - Pre-grasp approach: the tool starts approaching the pneumatic rail. II - Grasp Acquisition: the tool engages with the rail. III - Post-grasp transportation: the rail is transported towards the target location. IV - Placement: the rail is correctly positioned over the targeted organ.

gentle movements of the organ itself (repositioning). In Fig. 2 on the right side, it is possible to see a schematic representation of the different steps.

A hybrid control system has been formulated to deal with the different steps allowing the surgeon to interact and supervise the entire execution. In the execution of the first half of the task (pick and place) we use a flexible approach which relies on gradient-based method. While once the *placement* is reached, the robotic arm is trained on the tissue repositioning and the aim is to construct a learning algorithm to improve the execution of the task taught via teleoperation. A preliminary study was executed to validate how the pressure applied through the rail in active suction can affect the tissue morphology. This will lead the foundations for future *in vivo* trials and further analysis. All the experiments have been executed with *ex vivo* porcine kidneys, with the future aim of extending the work to other organs (liver, bowel).

The algorithms were developed based on the following assumptions:

- The effects of the blood pressure as well as of the physiological motion are not considered given that all the experiments have been conducted on *ex vivo* organs.
- Visual feedback of the robot and tissue features are always available. The rail, and the organs features are never occluded.

Further studies will be carried out to understand the tolerance due to the suction power and whether this is compatible with the kidney motion [30].

The remainder of the paper is organized as follows: in section IV there are the main algorithm contributions: calibration and visual feedback, gradient-based planning and similar

smooth path repositioning along with the description of the experimental setup. Section V contains the experimental evaluation and results from the experiment: *A. Validation of the pressure level*, *B. Pick, place and relocate configurations* and *C. Results*. The paper concludes, section VI, with a discussion of results and some planned future work.

## IV. METHODOLOGY

### A. Calibration and Visual Feedback

A crucial prerequisite for the successful execution of a task where robot and surgeon collaborate in unstructured environments is the perception of the environment from each side and how those perceptions can be merged together. Calibration enables communication among the different actors involved. As shown in Fig. 2 on the left, the system is characterized by different reference frames. The stereo endoscope has been calibrated using Zhang's method [31]. For the remaining transformations, a specific point cloud has been selected, and knowing the coordinate of each point in the different reference frames, the calibration problem can be formulated as a point cloud registration problem [29].

The vision system presents an interface which allows the surgeon to select the position of the PAF rail and the location where it should be placed on the organ surface. The selection of the grasping site represents the input of the entire system. The coordinates of the selected point are then triangulated and reconstruct in the 3D space and use as the target of the pick and place task since all the transformation among reference frames are known. In parallel, in order to process the final targeted position, the reconstruction of the kidney surface is needed. Hence, the kidney is segmented both in the left and right frame, following which local features are extracted using SURF algorithm [32] for both frames. The

two points clouds are triangulated, reconstructed, translated in the robot reference frame and used as the target for the placement phase.

### B. Control System

**Gradient-based planning** - The algorithm takes as input the position of the rail defined by the surgeon and allows the robot to grasp it and position it on the kidney's surface according to the surgeon's desire. Notably, the motion of the organ due breathing has not been considered. However, aiming at further developments, it has been decided to choose a planning algorithm based on a flexible approach to allow quick re-planning and to constrain some degrees of freedom.

For every step in time, starting from the current position of the tooltip in the Cartesian space, an intermediate position is computed using the gradient-based approach. This new position is located to a certain distance, *next-transl*, and if the target is within the next-translation distance, the new Cartesian position is the target itself. A similar computation is executed for the translation, where *next-rot* is calculated as the rotation necessary to convert the current orientation of the tooltip in the target one. The target orientation is defined along the x-axis (direction shown in Fig. 2 on the left side). Due to the PAF grasping site design, it is important to correctly grasp the rail with the tooltip in the proper orientation, to guarantee an effective grasp. Hence, after the grasp-acquisition step, the orientation is never more than a small angle away from the desire targeted organ surface orientation. We assume that the orientation of the rail in the operating area previous to grasp can be controlled by the surgeons assistance through the pressure pipe.

Using *cisst-saw* library [33], we compute the Cartesian Jacobian and angular velocity Jacobian, which show how changes in the joint angles effects the final pose of the tooltip in the Cartesian space. Rotations are given in angle-axis representation. The parameters *next-transl* and *next-rot* guarantee that the intermediate tool tip pose is "close" to the current one, so it is reasonably possible to linearize our problem to be the Equation 1, where  $J_{tr}$  and  $J_r$  are the Cartesian translation and rotation Jacobian defined above, and  $\Delta_r$  and  $\Delta_r$  the desired translation and rotation to move the end effector to the intermediate target. The da Vinci robotic arm has 6 DoF and ordinary least-squares regression is used to compute the required joint changes necessary to satisfy the equation.

$$\begin{bmatrix} J_{tr} \\ J_r \end{bmatrix} \Theta = \begin{bmatrix} \Delta_r \\ \Delta_r \end{bmatrix} \quad (1)$$

**Similar Smooth Path Repositioning** - The problem addressed is how to actually validate if the system can be applied for doing organ repositioning and tissue retraction. Since it is a completely new design, no real clinical protocol is available in the literature regarding this application. For this reason, it has been decided to use expert knowledge to teach the robot how to perform repositioning manoeuvres.

Given  $\Gamma$  as the set of valid configurations  $\Gamma = (\gamma_1, \gamma_2, \dots, \gamma_n) \in \mathbb{R}^n$  where  $n$  is the number of degrees of

freedom of the robotic arm and  $\gamma_i$  is the parameterization of the  $i^{th}$  degree of freedom. The trajectory is defined as a set pairs of joint states and times,  $\{(\gamma_1, t_1), \dots, (\gamma_k, t_k)\}$ , where  $\gamma_i \in \Gamma$ ,  $t_i \in \mathbb{R}$ , and  $t_i < t_{i+1}$ . The entire set of trajectories is represented by  $\Psi$ . Since the robot is trained via tele-operation, the training demonstration is an element of the set  $\Psi$ . Assuming  $C: \Psi \rightarrow \mathbb{R}$  some existing cost function known to the robot, that gives a measure of the cost of any trajectories. This  $C$  could be any cost, like the energy needed to achieve that trajectory, the total path length, the smoothness of the path. It is assumed that the controller knows some task-success-evaluation function  $S: \Psi \rightarrow \{0, 1\}$ , which is able to tell whether a trajectory satisfactorily completes the task, in which case  $S$  returns 1, or not, in which case  $S$  returns 0. The  $S$  function is evaluated by a control step based on the visual feedback: if the robot is actually able to establish a correct suction with the organ for the whole execution of the movements, the task is considered successful. If the PAF rail correctly gets in suction with the organ surface but when the tool tries to lift the organ the suction is lost, the task is considered failed. The robot is able to ask the control system to evaluate the success function  $S(\Psi)$  for any trajectory  $\Psi$ . Every time the robot asks for a trajectory evaluation, it actually has to execute the trajectory and each time the control system evaluates a trajectory is a learning step. Pursuant to [34], we consider to enhance the learning problem introducing the control signal based on the visual feedback of the robot without the need of having a physical teacher acting as a controller. The problem is defined as follow: the robot is shown a single trajectory  $\psi_d \in \Psi$  via tele-operation by the surgeon. The robot asks the control feedback to evaluate the success of  $N$  different trajectories. The robot's learning problem is to find, after this learning steps a learned trajectory  $\psi_l$  for which  $S(\psi) = 1$  and which makes  $C(\psi_d) - C(\psi_l)$  as large as possible.

Under a safety perspective, exploring new trajectory with a robot in the real world can be dangerous. Using a learning algorithm that improves the trained trajectory via teleoperation reduces the risks. More concretely, as shown in the Algorithm 1 below, the robot first defines a function  $d: \Psi \rightarrow \mathbb{R} \geq 0$  that measures how different a new trajectory is from the demonstrated one ( $d$  only defines a notion of distance from the training trajectory). Secondly, the robot picks some distance parameter  $\delta_{now} \in \mathbb{R}$  and searches over the set of trajectories  $\{\psi \mid d(\psi) < \delta_{now}\}$  for the trajectory in that set that minimizes the cost  $C(\psi)$ .

The robot then performs a learning step and asks the control feedback if that trajectory is successful. A single learning step covers the execution of different movements mimicking the repositioning task (the different steps are shown in Fig. 3). The position of the kidney surface, engaged in suction with the rail, is used as control signal. Hence, after each of those movements, the controller acquires two new frames, detects and reconstructs the new position of the organ surface. If it is above a threshold distance compared with the initial position during all the different movements, the trajectory is considered successful. If the trajectory is

**Algorithm 1:** SSPP - Similar Smooth Path Repositioning

---

**Result:** Return  $\Psi_{current-best}$

- 1 Initialize  $\Psi_{current-best}$  to the trained trajectory;
- 2 Initialize  $\delta_{min} \leftarrow 0$ ;
- 3 Initialize  $\delta_{now}$  to some arbitrary value;
- 4 Initialize  $\Delta_{MaxKnown} \leftarrow False$ ;
- 5 iteration  $\leftarrow 0$ ;
- 6 **while** iteration  $< N$  **do**
- 7     **if**  $\Delta_{MaxKnown}$  **then**
- 8          $\delta_{now} \leftarrow (\delta_{min} + \delta_{max})$ ;
- 9     **else**
- 10          $\delta_{now} \leftarrow \delta_{now} * 2$ ;
- 11     **end**
- 12     Define similar trajectories  $\Psi_{\delta} = \{\psi \mid d(\psi) < \delta_{now}\}$
- 13      $\Psi_{test} \leftarrow \arg \min_{\psi \in \Psi_{\delta}} C(\psi)$ ;
- 14     Ask the control feedback to evaluate  $success \leftarrow S(\Psi_{test})$ ;
- 15     **if**  $success$  **then**
- 16          $\delta_{current-best} \leftarrow \Psi_{test}$ ;
- 17          $\delta_{min} \leftarrow \delta_{now}$ ;
- 18     **else**
- 19          $\delta_{max} \leftarrow \delta_{now}$ ;
- 20          $\Delta_{MaxKnown} \leftarrow True$ ;
- 21     **end**
- 22     **if** *The robot receives additional feedback* **then**
- 23         The robot updates  $d$  based on that feedback;
- 24     **else**
- 25     **end**

---

successful, the robot increases  $\delta_{now}$  and repeats. If the trajectory is not successful, the robot decreases  $\delta_{now}$  and repeats. If the robot is given information about particular parts of the trajectory that led to failure, the robot may also update the distance function  $d$  to make the trajectory more closely align to the training trajectory for those failing time steps. The aim of this algorithm is to make the robot focusing on the search of trajectories that are likely to improve the cost function  $C$ . We expect this algorithm to be robust to the choice of the initial  $\delta_{now}$ , as it performs an exponential search in the  $\delta$  parameter. For safety reasons, to avoid the robot executing dangerous trajectories, we suggest that  $\delta_{now}$  be initialized to a small value.

## V. EXPERIMENTAL EVALUATION AND RESULTS

### A. Validation of the pressure level

Few devices applying suction pressure to organ surfaces have been used in clinical practice. As a preliminary step, we decided to validate which are the possible outcomes of applying continuous suction pressure to tissue samples with the aim to plan for future *in vivo* experiments. We used a 3CFM single stage vacuum pump (Bacoeng, Hawthorne, CA) vacuumises a 12-liters vacuum chamber (Bacoeng, Hawthorne, CA). The vacuum chamber is used as a vacuum tank to monitor the pressure with the embedded manometer.

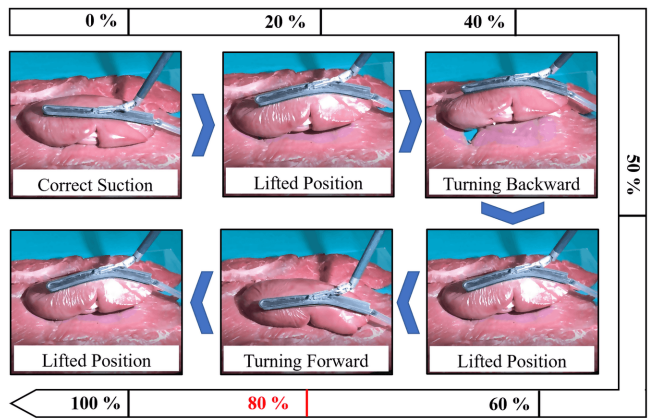


**Fig. 3:** Representation of the different movements mimicking the repositioning task. Each learning step is made by the execution of all the six movements. After every single step the position of the kidney is detected to verify if the suction is still active. The execution of 80% of the task is considered successful. If the suction is lost before this value is reached, the task is considered failed.

**TABLE I:** Results from preliminary *ex vivo* experiments in pig kidneys.

| Pressure  | Time   | Morphological Disruption | Disruption distance from margin in $\mu\text{m}$ |
|-----------|--------|--------------------------|--------------------------------------------------|
| 3.325kPa  | 5 min  | Absent                   | NA                                               |
| 7.325kPa  | 5 min  | Absent                   | NA                                               |
| 11.325kPa | 5 min  | Absent                   | NA                                               |
| 3.325kPa  | 30 min | Present                  | 100                                              |
| 7.325kPa  | 30 min | Absent                   | NA                                               |
| 11.325kPa | 30 min | Present                  | 100                                              |
| 3.325kPa  | 60 min | Present                  | 100                                              |
| 7.325kPa  | 60 min | Present                  | 150                                              |
| 11.325kPa | 60 min | Present                  | 200                                              |

A pressure line (PVC) pipe connects the chamber with the tested PAF rail (Fig. 2).

To investigate the effects of applying suction pressure over time in internal organs, we conducted a preliminary *ex vivo* experiment in pig kidneys. These organs frequently need to be mobilised intra-operatively. We arbitrary decided to test three set of times,  $t_1=5 \text{ min}$ ,  $t_2=30 \text{ min}$ ,  $t_3=60 \text{ min}$ , and three different value of pressures,  $P_1=3.325 \text{ kPa}$ ,  $P_2=7.325 \text{ kPa}$ ,  $P_3=11.325 \text{ kPa}$ . The pressure values have been chosen as a trade off between the pressure values reachable with our vacuum pump, and the ones reachable with pumps in the

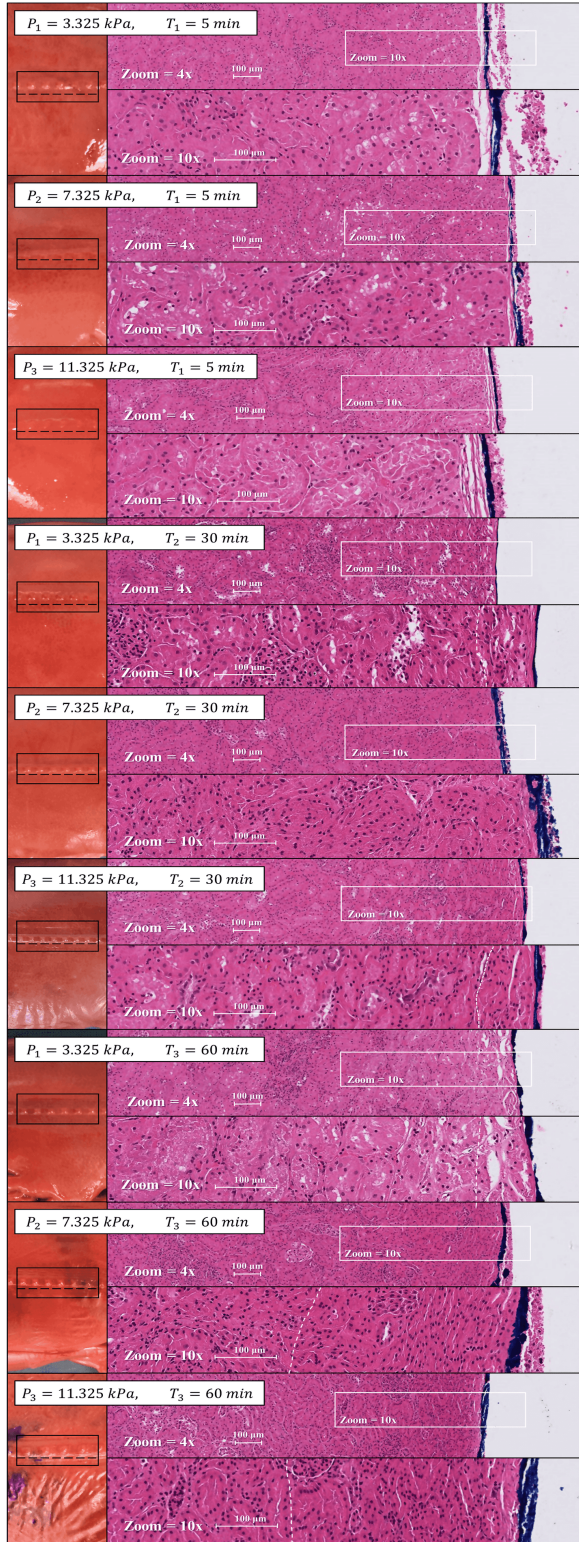


**Fig. 4:** Samples obtained from all the different tests. In the first block, the pressures  $P_1=3.325kPa$ ,  $P_2=7.325kPa$ ,  $P_3=11.325kPa$  have been applied for  $T_1=5$  min. In the second, the application time is 30 min, while in the last block 60 min. On the left side, samples of kidney microscopically shows the consequences of applied the suction force over the tissue. The black squares locates the area have been resected for the analysis.

surgical theatre. The margin in contact with the PAF rail was inked blue and a section of tissue was embedded in paraffin. Tissue sections ( $5 \mu\text{m}$ ) were taken and morphology assessed using haematoxylin and eosin (H & E) stain. Visual estimation was used to analyse the stained tissue sections. Samples were categorised according to the presence or absence of disruption of normal morphology at the contact margin at 4x and 10x magnification. If disruption was present, the average affected distance from margin to normal tissue was assessed. Assessment was done by two independent researchers, disagreement was resolved by consensus. Results are presented in TABLE I.

After a couple of trials in executing the task in teleoperation, as a good trade-off, we decide to use  $P_{medium}=7.325kPa$  for the experiments. This value could guarantee active suction throughout the entire execution of the task by the expert. This was a proof of concept experiment and future plans include *in vivo* experiments to assess microvasculature and structural disruption, and inflammatory infiltration. this would include immunohistochemistry for endothelial markers (such as CD31 and CD34), and local inflammatory infiltration (using CD45, CD3 and other relevant markers), and markers of fibrosis (e.g. vimentin).

### B. Experimental Configuration

Experiments were performed on a first generation da Vinci Surgical System with the dVRK controllers. The Patient Side Manipulator (PSM) is equipped with the ProGrasp tool. The PAF rail prototype is connected to the vacuum tank as described above and is manually located inside the field of view of the endoscope, its orientation can be controlled through the pressure line, Fig.2.

In these experiments, for the repositioning task, the minimization of the roughness (sum of squared second derivative) of the trajectory has been chosen as cost function. As constrain instead, the square root of the weighted average square distance between the new path and the old path over all time-stamps is less than the constraint distance. Natural cubic spline can be used to solve the smoothness function combined with the distance one [35]. The choice of roughness as a cost function comes from the need to guarantee active suction during the entire execution of the task. Jerky trajectories will increase the inertia applied to the kidney, leading to the need for applying higher pressure through the vacuum pump.

The surgeon executes the task via teleoperation a sampled movement for testing the organ repositioning. First, the kidney is lifted and then tilted around the axis connecting the upper and lower poles, forward and backward. A representation of the different steps can be visualized in Fig. 3. This protocol has been chosen based on the most common movements during the surgical practice. Indeed, the challenging part is being able to lift and tilt the organ to check the conditions of the tissue posterior areas, which are normally outside the operational field of view.

The experiment acquisition starts with the surgeon selecting through the interface the position of the trail to be grasped

and the desired target location over the organ surface. The hybrid control system first executes the pick and locate task, using as input the variables determined by the surgeons. Subsequently, the robot performs the learned trajectory and at each step of the SSPR algorithm we optimize the cost function using [36], given the  $\delta$  constrain.

When the surgeon executes the repositioning task in teleoperation, the rail stays on suction for the whole execution. For each execution, we define a score in percentage which represents for how long during the execution an active suction is maintained between the organ and the PAF rail. The whole execution of the task represents 100 %, the full sequence is shown in Fig.3. We consider the robot failing the task if the kidney drops before concluding the tilting in both directions (80% execution).

### C. Pick and Place Task Results

We initialize the  $\delta$  to 0.01 radians (1 millimeter for the translational one). After nine steps of the learning algorithm, the  $\delta$  bounded between 0.016 and 0.01688 radians (2.3 and 2.8 millimeter). We compute the total sum of squared second derivatives (the cost function), in order to quantify how much SSPR algorithm was able to optimize the trained trajectory. The training trajectory had a total cost of 2.78 radians/second<sup>2</sup>, while the learned one 0.235 radians/second<sup>2</sup>, showing improvement over the cost function. Using the newly learned trajectory we execute one more time the repositioning task and due to the improved smoothness, we were able to decrease the pressure level from  $P_2=7.325\text{kPa}$  minimum value required in teleoperation, to  $P_3=11.325\text{kPa}$ .

## VI. CONCLUSION AND FUTURE WORK

In this paper, a first proof of concept for a new PAF device is presented. This can potentially aid in organ repositioning and retraction during RAMIS. In preliminary *ex vivo* experiments, analysis were able to assess microscopic morphological changes in tissue structure over a range of suction forces and time applied. Thanks to the performance of the SSPR algorithm the demonstrated trajectory is improved, decreasing the minimum level of pressure necessary to execute the entire task with effective suction. Further developments will focus on studies about the interaction of the system with the organ surfaces, especially focusing on assessing microvasculature disruption, inflammatory infiltration and acute and chronic reactionary changes. From the algorithmic point of view, better tracking of the organ will be integrated in order to be able to achieve faster computation which will allow to take into account breathing motions. Situations with partial occlusion will also be taken into account. There is also the hope to further develop the hybrid control algorithm in order to reach a better integration and to be able to control the robot not only in the joint space but also in Cartesian space.

## REFERENCES

- [1] "Frequently Asked Questions," 2019. [Online]. Available: <https://www.davincisurgery.com/da-vinci-gynecology/da-vinci-surgery/frequently-asked-questions.php>
- [2] A. Stilli, E. Dimitrakakis, C. D'Ettoire, M. Tran, and D. Stoyanov, "Pneumatically Attachable Flexible Rails for Track-Guided Ultrasound Scanning in Robotic-Assisted Partial Nephrectomy: A Preliminary Design Study," *IEEE Robotics and Automation Letters*, vol. 4, no. 2, pp. 1208–1215, 2019.
- [3] "Inferior Vena Cava (IVC) Thrombectomy - da Vinci Robotic Surgery." [Online]. Available: <https://www.youtube.com/watch?v=5JM8KhWhrus>
- [4] Y. Duan, M. Andrychowicz, B. C. Stadie, J. Ho, J. Schneider, I. Sutskever, P. Abbeel, and W. Zaremba, "One-Shot Imitation Learning," 2017.
- [5] B. D. Argall, S. Chernova, M. Veloso, and B. Browning, "A survey of robot learning from demonstration," *Robotics and Autonomous Systems*, vol. 57, no. 5, pp. 469–483, 2009.
- [6] B. Argall, B. Browning, and M. Veloso, "Learning robot motion control with demonstration and advice-operators," in *2008 IEEE/RSJ International Conference on Intelligent Robots and Systems*, 2008, pp. 399–404.
- [7] J. H. Khan, R. K. Wolf, W. D. Fox, G. W. Knight, D. L. Hamann, and C. B. Berky, "Method for using a tissue stabilization device during surgery," 2000.
- [8] W. D. Fox, D. L. Hamann, C. B. Berky, and G. W. Knight, "Tissue stabilization device for use during surgery having remotely actuated feet," 1999.
- [9] F. J. Benedetti, C. S. Taylor, I. Sepetka, A. Salahieh, R. C. Glines, W. N. Aldrich, B. Regan, and J. J. Frantzen, "Surgical method for stabilizing the beating heart during coronary artery bypass graft surgery," 1999.
- [10] C. Taylor, F. Benetti, and R. Matheny, "Surgical devices for imposing a negative pressure to stabilize the cardiac tissue during surgery," 1999.
- [11] A. Jadhav, R. Rodke, and Y. Vikharankar, "Surgical instruments for engaging tissue to stabilize tissue and facilitate tissue manipulation," 2019.
- [12] W. Tamara and S. Frederick, "Surgical bowel retractor devices," 2019.
- [13] B. D. Argall, S. Chernova, M. Veloso, and B. Browning, "A survey of robot learning from demonstration," *Robotics and Autonomous Systems*, vol. 57, no. 5, pp. 469–483, may 2009.
- [14] G. Ye and R. Alterovitz, "Demonstration-Guided Motion Planning," 2017, pp. 291–307.
- [15] C. E. Reiley, E. Plaku, and G. D. Hager, "Motion generation of robotic surgical tasks: Learning from expert demonstrations," in *2010 Annual International Conference of the IEEE Engineering in Medicine and Biology*, 2010, pp. 967–970.
- [16] J. van den Berg, S. Miller, D. Duckworth, H. Hu, A. Wan, Xiao-Yu Fu, K. Goldberg, and P. Abbeel, "Superhuman performance of surgical tasks by robots using iterative learning from human-guided demonstrations," in *2010 IEEE International Conference on Robotics and Automation*, 2010, pp. 2074–2081.
- [17] T. Osa, N. Sugita, and M. Mitsuishi, "Online Trajectory Planning in Dynamic Environments for Surgical Task Automation," in *Robotics: Science and Systems X*. Robotics: Science and Systems Foundation, 2014.
- [18] J. Schulman, A. Gupta, S. Venkatesan, M. Tayson-Frederick, and P. Abbeel, "A case study of trajectory transfer through non-rigid registration for a simplified suturing scenario," in *2013 IEEE/RSJ International Conference on Intelligent Robots and Systems*, 2013, pp. 4111–4117.
- [19] H. Mayer, I. Nagy, D. Burschka, A. Knoll, E. U. Braun, R. Lange, and R. Bauernschmitt, "Automation of Manual Tasks for Minimally Invasive Surgery," in *Fourth International Conference on Autonomic and Autonomous Systems (ICAS'08)*. IEEE, 2008, pp. 260–265.
- [20] A. Murali, S. Sen, B. Kehoe, A. Garg, S. McFarland, S. Patil, W. D. Boyd, S. Lim, P. Abbeel, and K. Goldberg, "Learning by observation for surgical subtasks: Multilateral cutting of 3D viscoelastic and 2D Orthotropic Tissue Phantoms," in *2015 IEEE International Conference on Robotics and Automation (ICRA)*, 2015, pp. 1202–1209.
- [21] A. Billard, S. Calinon, R. Dillmann, and S. Schaal, "Robot Programming by Demonstration," in *Springer Handbook of Robotics*. Springer Berlin Heidelberg, 2008, pp. 1371–1394.
- [22] S. Riazzi, K. Bengtsson, O. Wigstrom, E. Vidarsson, and B. Lennartson, "Energy optimization of multi-robot systems," in *2015 IEEE International Conference on Automation Science and Engineering (CASE)*. IEEE, 2015, pp. 1345–1350.
- [23] L. Thomas and Doersam, "Robotic hands: modelisation, control and grasping strategies," 1996.

- [24] W. Qian, Z. Xia, J. Xiong, Y. Gan, Y. Guo, S. Weng, H. Deng, Y. Hu, and J. Zhang, "Manipulation task simulation using ROS and Gazebo," in *2014 IEEE International Conference on Robotics and Biomimetics (ROBIO 2014)*. IEEE, dec 2014, pp. 2594–2598.
- [25] C. Zito, R. Stolkin, M. Kopicki, and J. L. Wyatt, "Two-level RRT planning for robotic push manipulation," in *2012 IEEE/RSJ International Conference on Intelligent Robots and Systems*. IEEE, 2012, pp. 678–685.
- [26] J. Zhu, B. Navarro, P. Fraisse, A. Crosnier, and A. Cherubini, "Dual-arm robotic manipulation of flexible cables," in *2018 IEEE/RSJ International Conference on Intelligent Robots and Systems (IROS)*, 2018, pp. 479–484.
- [27] F. Chen, M. Selvaggio, and D. G. Caldwell, "Dexterous Grasping by Manipulability Selection for Mobile Manipulator With Visual Guidance," *IEEE Transactions on Industrial Informatics*, vol. 15, no. 2, pp. 1202–1210, 2019.
- [28] F. Alambeigi, Z. Wang, R. Hegeman, Y.-H. Liu, and M. Armand, "Autonomous Data-Driven Manipulation of Unknown Anisotropic Deformable Tissues Using Unmodelled Continuum Manipulators," *IEEE Robotics and Automation Letters*, vol. 4, no. 2, pp. 254–261, 2019.
- [29] C. D’Ettorre, G. Dwyer, X. Du, F. Chadebecq, F. Vasconcelos, E. De Momi, and D. Stoyanov, "Automated Pick-Up of Suturing Needles for Robotic Surgical Assistance," in *2018 IEEE International Conference on Robotics and Automation (ICRA)*. IEEE, 2018, pp. 1370–1377.
- [30] D. Pham, T. Kron, F. Foroudi, M. Schneider, and S. Siva, "A Review of Kidney Motion under Free, Deep and Forced-Shallow Breathing Conditions: Implications for Stereotactic Ablative Body Radiotherapy Treatment," *Technology in Cancer Research & Treatment*, vol. 13, no. 4, pp. 315–323, 2014.
- [31] Z. Zhang, "A flexible new technique for camera calibration," *IEEE Transactions on Pattern Analysis and Machine Intelligence*, vol. 22, no. 11, pp. 1330–1334, 2000.
- [32] H. Bay, T. Tuytelaars, and L. Van Gool, "SURF: Speeded Up Robust Features," 2006, pp. 404–417.
- [33] P. Kazanzides, Z. Chen, A. Deguet, G. S. Fischer, R. H. Taylor, and S. P. DiMaio, "An open-source research kit for the da Vinci® Surgical System," in *2014 IEEE International Conference on Robotics and Automation (ICRA)*. IEEE, 2014, pp. 6434–6439.
- [34] T. Rhodes and M. Veloso, "Robot-driven Trajectory Improvement for Feeding Tasks," in *2018 IEEE/RSJ International Conference on Intelligent Robots and Systems (IROS)*. IEEE, 2018, pp. 2991–2996.
- [35] P. Green and B. W. Silverman, *Nonparametric regression and generalized linear models: a roughness penalty approach*, C. Press, Ed., 1993.
- [36] C. H. Reinsch, "Smoothing by spline functions," *Numerische Mathematik*, vol. 10, no. 3, pp. 177–183, 1967.